COMBINED BENDING AND TORSIONAL FATIGUE OF WOVEN ROVING GRP

M.N. Aboul Wafa, A.H. Hamdy and A.A. El-Midany
Mechanical Engineering Department, Faculty of Engineering,
Alexandria University, Alexandria, Egypt.

ABSTRACT

A study of biaxial fatigue of woven roving glass reinforced polyester (GRP) subjected to in-phase and out-of-phase cyclic bending and torsional moments is presented. To evaluate failure theories for this material, tests are conducted on two fiber orientations [0,90] and [45,-45] tubes. The results showed that for [0,90] composites the S-N curves in pure bending and in pure torsion are sufficient to predict life. While, for [45,-45] tubes the value of the normal stress interaction component of a strength tensor H_{12} has to be obtained. If the ratio of the global flexural stress amplitude A to the accompanied global shear stress B is less than 2, the value of H_{12} may be taken as presented by Tsai-Hahn theory. But,if $A/B \geq 2$, the value of H_{12} has to be obtained from [45,-45] pure bending S-N curve,the reason is that the failure mode is a combination of interfacial shear and matrix failure. The out-of-phase loading results showed that the lives of the specimens at high stress levels are less than that for the in-phase loading with the same peak values A and B.

Keywords: Fatigue, Composite materials, Combined stress.

Nomenclature

σ_x	Global normal stress due to bending moment in the longitudinal direction.
A	Amplitude of σ_x.
τ_{xy}	Global shear stress due to torsion.
B	Amplitude of τ_{xy}
ωt	Angular displacement
Z	Phase shift
σ_1, σ_2, σ_6	Normal and shear stresses in the direction of the principal material axes.
F_{1t}, F_{1c}, F_{2t} , F_{2c}	Strength in the principal material directions (t for tension and c for compression).
F_6	Shear strength.
H_{12}	Normal stress interaction component of a strength tensor.

1. INTRODUCTION

The design of light weight structures requires the use of materials having high strength / density ratio, composite materials satisfy such requirements. In addition they should have sufficient resistance to fatigue loading when fluctuating loading conditions exist.

Although R.M. Jones [1], and many other investigators [2], [3] suggested that composite materials offer substantial improvement over metals in cyclic loading, more results and investigations are required to minimize the effect of the scatter in fatigue life data. P.C. Chow [4] reported that the fatigue life can vary by a factor of 1000 between the most and least durable ones. One can question this figure since this factor includes the effect of stiffness degradation in the absence of the failure definition. The amount of fatigue data on tubular specimens is quite limited [2]. Fatigue data of Woven roving glass/polyester composite tube is rather scarse.

M.J. Owen, et al., [5],[6], predict the biaxial stress failure surfaces for a glass fabric reinforced resin. They compared several failure criteria under hoop and axial stresses with zero shear stress. Their work included a failure contour for the onset of a damage in tubes at 10^6 cycles. In this contour the tension-tension region had values less than that of tension-compression region (about 50% in some cases). They

did not give any explanation.

In the present work, the failure contours for fatigue of woven roving GRP under combined bending and torsional loading are presented for two fiber orientations. It is our aim to find a fairly accurate and applicable failure criterion. The effect of stress state on the expected failure mode is also presented in-phase and out-of phase.

2 - EXPERIMENTAL WORK

Materials

Test specimens were made of woven roving E-glass (Product of the scandinavian fiber-glass Co., Sweden)/polyester tubes. The intensity of the glass fiber in both fill and warp directions is equal to 60 strands in each roving [ASTM D 2150-63]. The polyester resin is Siropol 8231. The properties of this resin are given in Table (1). This resin is prepromoted with special accelerators. Just prior to use the M.E.K. peroxide was added only at a level of two percent.

Table 1. Resin properties.

Viscosity Cps (25 deg.)	450
Percent styrene	40
Specific gravity	1.04
Gel time (25 deg.) (MINS)	25
Cure time (HRS)	3
Tensile elongation	1.7
Heat distortion temp. (resin)	70 deg.
Heat distortion temp. (Laminated)	200 deg.

Specimen Preparation

Sections of a woven roving sheet were cut from a roll of sufficient length to give two turns around a winding mandrel plus 5 mm for circumferential overlap. The width of the sheet was sufficient to cover the desired specimen length plus 30 mm to ensure a nearly void free part of the fabricated tube. It is obvious that the fiber direction was checked before cutting the glass sections from the roll. To avoid angular distortions, the ends of each section were fixed using cellutape before cutting. Figure (1), shows the wooden winding mandrel with the grippers of the fabricating machine. This mandrel was rotated slowly against a teflon rod free to rotate and secured to the fabricating machine through adjusting screw in order to control the gap between the teflon rod and the specimen. The resin was poured gradually during the rotation till the fibers were completely wet. Then the teflon rod was readjusted to roll out the surplus resin and to get rid of air bubbles. This operation took about 15 minutes. Another cellophane sheet was inserted between the winding mandrel and the teflon rod and was wrapped around the tube mandrel carefully to ensure a void free glazed surface. After two days, this sheet was removed. The tubes were cut to the desired length after removal from the mandrel and left for more than three weeks before testing to ensure stability of their mechanical properties.

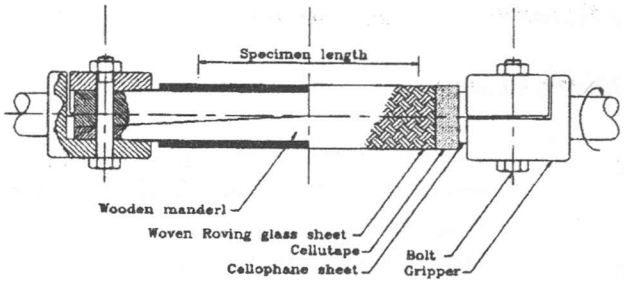

Figure 1. The winding mandrel covered with the woven roving glass sheet and the cellophane release film.

The glass content was kept 60% $\pm$ 4% by weight and was calculated by successive weighing of the mandrels with the release cellophane sheet then with the fiber then with the cured composite tube. Few burn tests were conducted to make sure that this procedure is accepted. Figure (2), shows the test specimen dimensions which were used here bearing in mind that there is no standardization of the specimen dimensions used in testing composite GRP tubes subjected to combined bending and twisting moments [7], [8] and [9].

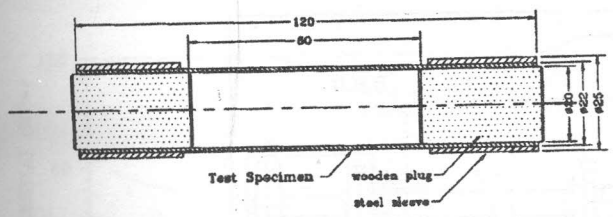

Figure 2. Test specimen dimension in mms.

The Testing Machine

The testing machine, Figure (3), designed to produce either pure bending, pure torsion or combined bending and torsion whether in-phase or out-of-phase. The machine is fully described in [10]. It consists of a driving pulley (13) connected to two couplings [12],[18]. Coupling [18] produces twisting moment through the connecting rod (8) with spring steel plates fastened to the twisting arm. This arrangement acts as a slider crank mechanism with a crank length equal to the eccentricity of the connecting arm which is controlled by means of a power screw inside the coupling. The rim of this coupling is adjustable to give a phase shift with respect to the left coupling (12). The intermediate shaft (9) is used to convert the axial displacement of the mechanism into equal displacements on the two bending arms (6). These displacements give uniform bending moment through the whole length of the specimen, Figure (4).

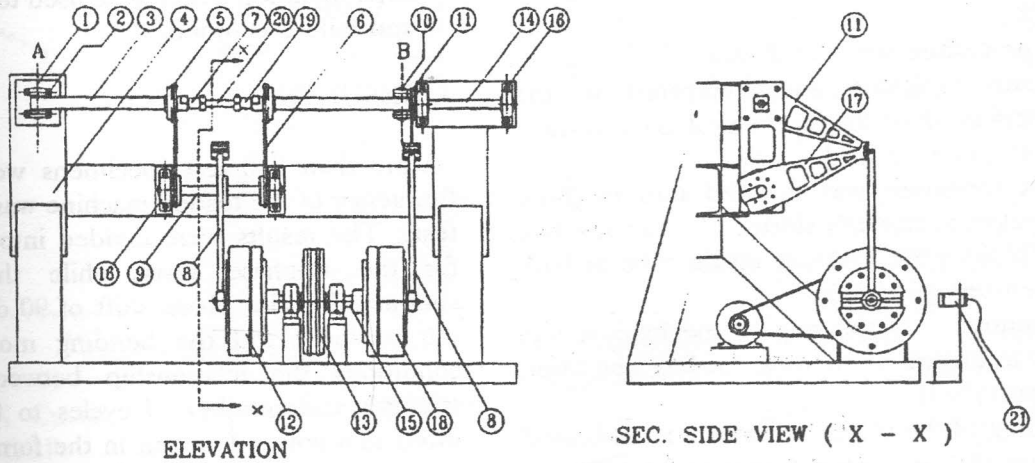

1. Supports A
2. Deep grove ball bearings
3. Specimen holder
4. Main frame
5. Self-aligning deep grove B. Br.
6. Bending arms
7. Bending Transducer
8. Connecting arm
9. Intermediate shaft
10. Supports B
11. Twisting arm
12. Bending coupling
13. Driving bulley
14. Guide shaft
15. Main shaft
16. Deep grove ball bearings
17. Loading arm
18. Torsion coupling
19. Torsion Transducer
20. Specimen
21. Proximity Switch

Figure 3 : General layout of the testing machine

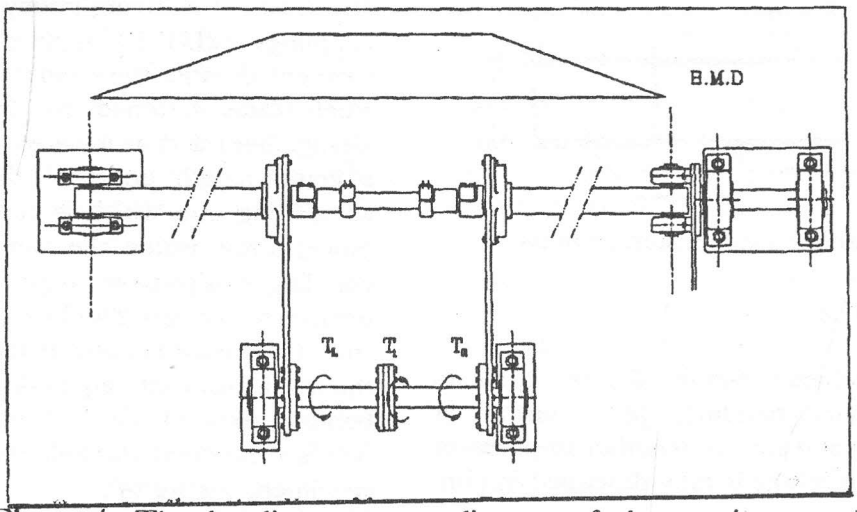

Figure 4. The bending moment diagram of the specimen and transducers.

Test Procedure

The test procedure was as follows:

1. The strain indicator was connected to the transducers to adjust the mechanical and electrical zero level under no load.
2. The test specimen was inserted into machine gripping system through slotted sleeves and two wooden plugs were inserted inside tube at both ends to ensure gripping.
3. The eccentricity of the engine mechanism was adjusted to ensure alternating loading condition (strain controlled).
4. The reading of the strain indicator was calibrated to measure the bending moment and torque.
5. The signal was transmitted to an oscilloscope to observe the change in strain amplitude.
6. The failure of the specimen was considered, if the strain reading was decreased by 20% of the original reading. This value is in accordance with Herrington et al. [11], to avoid the effect of stiffness degradation.
7. At this stage the electronic counter had recorded the number of cycles through the proximity switch (21) and the failure was checked. If the failure was out of the gauge length, the result of this specimen was dropped because the crack may be initiated under the grip due to heavy tightening.
8. The resulting number of cycles and the corresponding stress were used to plot S-N curves and failure contours.

3. RESULTS

More than 230 test specimens were tested. The frequency of the testing machine was 16.7 HZ for all tests. The results were divided into two group,one for the in-phase tests, while the other were conducted under phase shift of 90 degree between the torsional and the bending moments. For all conditions the relationship between the fatigue strength and number of cycles to failure N was fitted to a power function in the form

$$\sigma = C1\ N^{-c2}$$

Where: C1,C2 are the constants of the S-N curve fitting in each case.

Table (2), shows values of C1 , C2 and the corresponding stress state for each curve. Figures (5) to (8) represent the S-N curves for pure bending and pure torsion for each fiber orientation, while Figures (9) to (14), show comparison between the in-phase and the out-of-phase S-N curves having the same peak values of A and B.

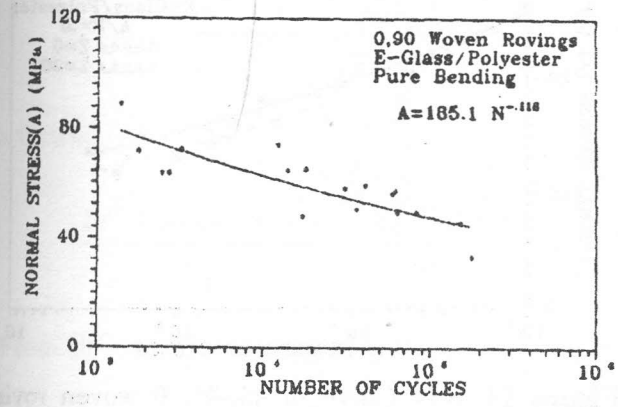

Figure 5. S-N Curve for pure bending of 0.90 woven roving GRP.

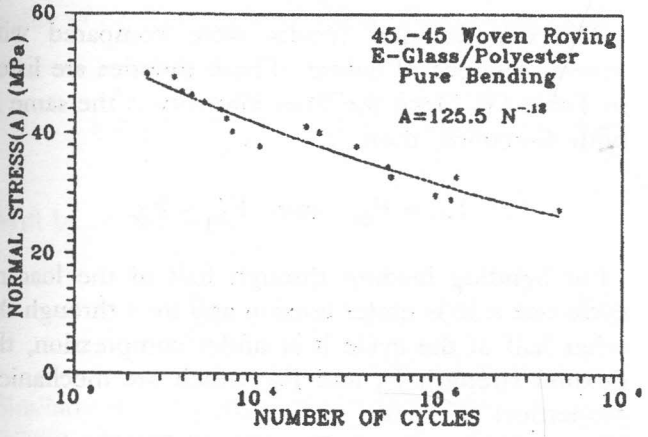

Figure 6. S-N Curve for pure bending of 45,45 woven roving GRP.

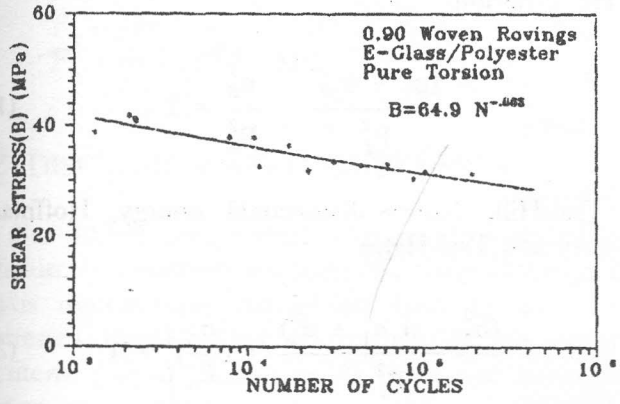

Figure 7. S-N Curve for pure torsion of 0.90 woven roving GRP.

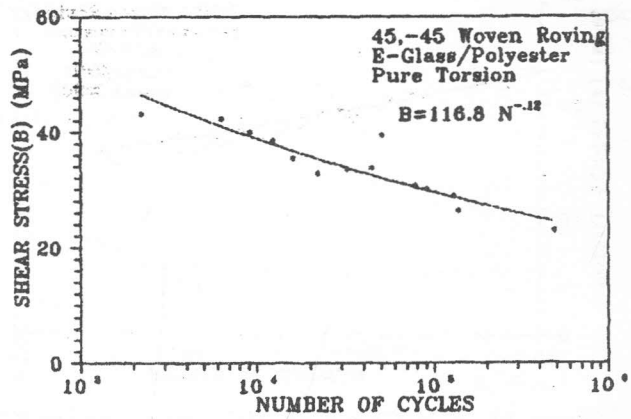

Figure 8. S-N Curve for pure torsion of 45,-45 woven roving GRP.

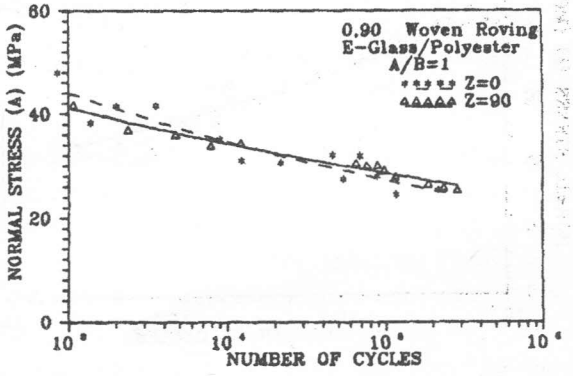

Figure 9. S-N Curve of 0,90 woven roving GRP in-phase and out-of-phase for A/B=1.

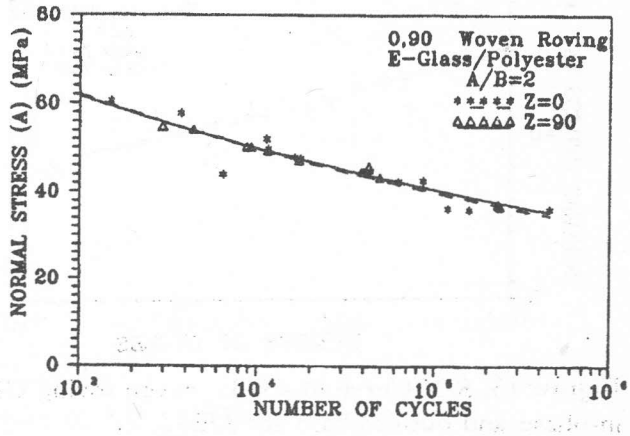

Figure 10. S-N Curve of 0,90 woven roving GRP in-phase and out-of-phase for A/B=2.

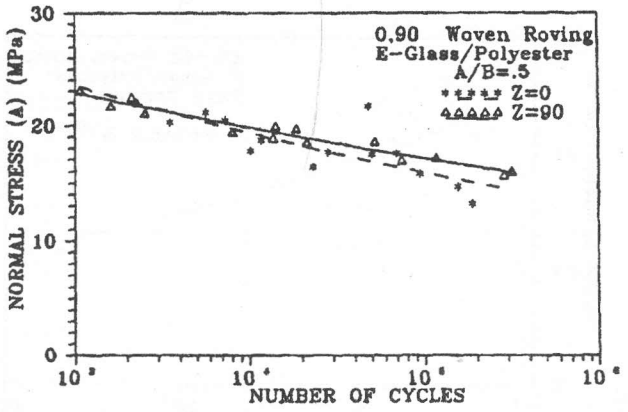

Figure 11. S-N Curve of 0,90 woven roving GRP in-phase and out-of-phase for A/B=0.5.

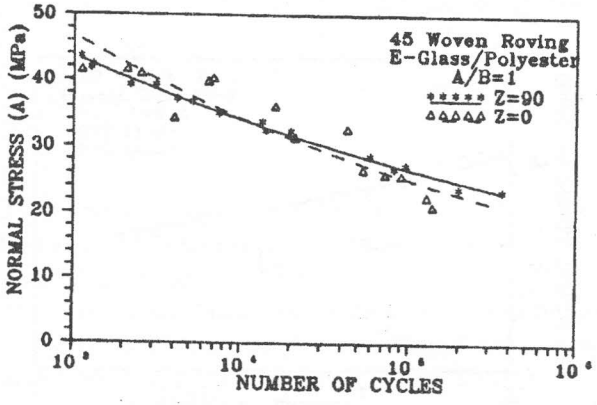

Figure 12. S-N Curve of 45,-45 woven roving GRP in-phase and out-of-phase for A/B=1.

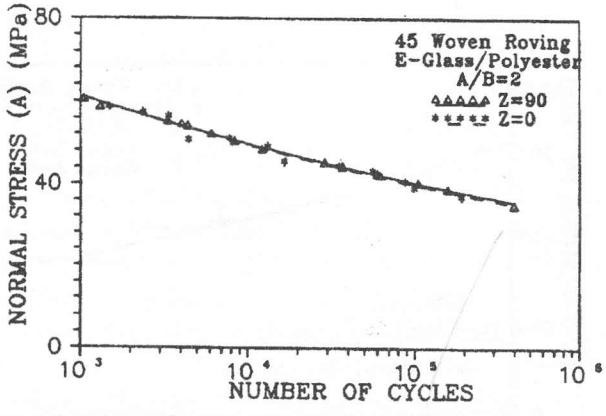

Figure 13. S-N Curve of 45,-45 woven roving GRP in-phase and out-of-phase for A/B=2.

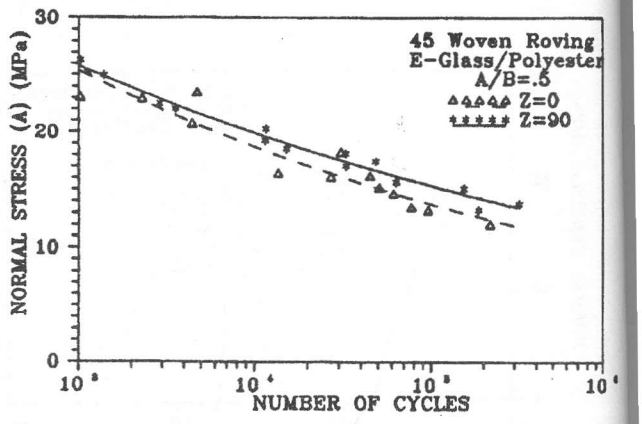

Figure 14. S-N Curve of 45,-45, 0 woven roving GRP in-phase and out-of-phase for A/B=0.5.

4- THEORETICAL ANALYSIS

The experimental results were compared with several theories of failure. These theories are listed in Table (3). Since the fiber intensity is the same in both directions, then

$$F_{1t} = F_{2t} \quad \text{and} \quad F_{1c} = F_{2c}$$

For bending loading through half of the loading cycle one side is under tension and then through the other half of the cycle it is under compression, the flexural strength F_1 and F_2 (which are mechanical properties) are used .
Then replacing F_{1t}, F_{1c} by F_1 and F_{2t}, F_{2c} by F_2 or F_1
The previous theories will be reduced to four criteria

- Hill criterion

$$\frac{(\sigma_1 - \sigma_2)^2}{F_1^2} + \frac{\sigma_6^2}{F_6^2} = 1 \qquad (1)$$

- Tsai-Hill, Norris distortional energy, Hoffman theory and,Tsai-Hahn

$$\frac{(\sigma_1^2 - \sigma_1\sigma_2 + \sigma_2^2)}{F_1^2} + (\frac{\sigma_6}{F_6})^2 = 1 \qquad (2)$$

- Norris and Mckinnon

$$\frac{\sigma_1^2 + \sigma_2^2}{F_1^2} + \frac{\sigma_6^2}{F_6^2} = 1 \qquad (3)$$

- Cowin

$$\frac{(\sigma_1^2 + 2\sigma_1\sigma_2 + \sigma_2^2)}{F_1^2} + \frac{\sigma_6^2 - \sigma_1\sigma_2}{F_6^2} = 1 \qquad (4)$$

From [0,90] pure bending test, the stress state is

$$\sigma_1 = A \quad \text{and} \quad \sigma_2 = \sigma_6 = 0$$

Substituting with these values in any of the theories of failure listed in table 3, will give the value of F_1. For example, the Tsai-Hill yield criteria.

$$(\frac{\sigma_1}{F_1})^2 - \frac{\sigma_1\sigma_2}{F_1^2} + (\frac{\sigma_2}{F_2})^2 + (\frac{\sigma_6}{F_6})^2 = 1$$

Will be in the form

$$(\frac{A}{F_1})^2 - 0 + 0 + 0 = 1$$

Similarly [0,90] pure torsion will give F_6. Now, the failure contours representing each of the previous theories can be drawn since F_1 and F_6 are given as functions of life N. Referring to the values in table 2.

$$F_1 = 185.1\ N^{-0.118}\ \text{MPa}$$
$$F_6 = 64.9\ N^{-0.063}\ \text{MPa}$$

5- DISCUSSION AND CONCLUSION

For [0,90] composites, Figure (15), shows the failure contours as constant life diagrams with the axis representing the global bending and shear stresses. For this fiber arrangement all the previous criteria give the same result since the interaction term $\sigma_1\ \sigma_2$ is always equal to zero because $\sigma_2 = 0$ in all conditions. It is also clear that the experimental results are generally in good agreement with the theoretical values especially at longer lives therefore, dealing with [0,90] woven roving GRP under combined bending and torsion requires only two S-N curves to get F_1 and F_6 and then the failure contour is obtained.

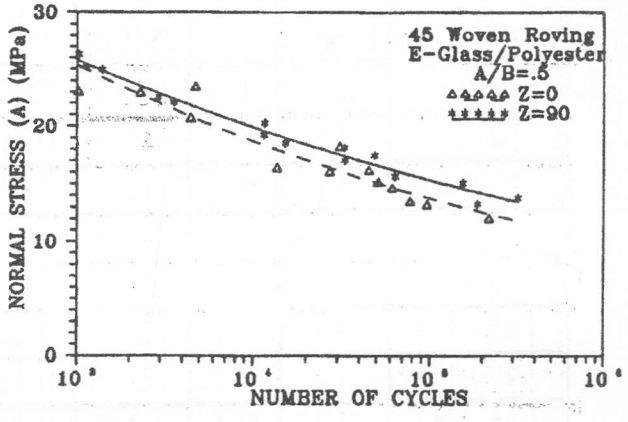

Figure 15. Theoretical and experimental failure contour of 0.90 woven roving GRP.

For [45,-45] tubes, the failure contour is quite different as shown in Figure (16) except for a specific point where A/B=2. Mentioning that at this point the stress state is the same for [0,90] and [45,-45] as shown in table 2. The results of the two S-N curves with A/B=2 for [0,90] and [45,-45] had nearly the same values which prove that the experimental work is quite well.

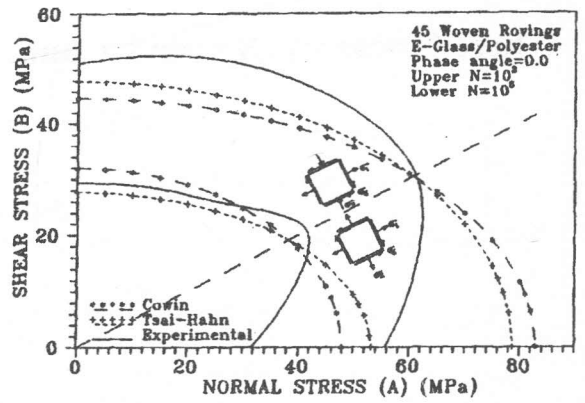

Figure 16. Theoretical and experimental failure contours of [45-45] woven roving GRP.

It is observed that this contour may be divided into two regions:

Table 2- Test Results and Stress State

Fiber Orientation	No. of Points	A/B	C1 (MPa)	C2	Z (deg.)	Stress State σ1	σ2	σ6
[0,90]	18	1/0	185.1	0.12	0	A	0	0
[0,90]	15	0/1	64.9	0.06	0	0	0	B
[0,90]	13	0.5	42.5	0.09	0	A	0	2A
[0,90]	13	1	89.9	0.1	0	A	0	A
[0,90]	13	2	120.2	0.1	0	A	0	A/2
[45,-45]	19	1/0	125.5	0.12	0	A/2	A/2	A/2
[45,-45]	14	0/1	116.8	0.12	0	B	-B	0
[45,-45]	13	0.5	63.5	0.13	0	2.5A	-1.5A	A/2
[45,-45]	14	1	119	0.14	0	1.5A	-A/2	A/2
[45,-45]	13	2	117.1	0.09	0	A	0	A/2
[0,90]	15	0.5	35.4	0.06	90	AS	0	2AC
[0,90]	13	1	68.2	0.08	90	AS	0	AC
[0,90]	13	2	115.3	0.09	90	AS	0	.5AC
[45,-45]	15	0.5	56.3	0.11	90	.5AS+2AC	5AS-2AC	.5AS
[45,-45]	17	1	91	0.11	90	.5AS+AC	.5AS-AC	.5AS
[45,-45]	15	2	114.5	0.09	90	.5AS+.5AC	5AS-.5AC	.5AS

Where C =cos wt , S = sin wt and wt is the angular position.

Table 3: Failure theories

	Name and Refernce	Failure Criterion
1	Hill criterion (Hill)[12]	$\left(\frac{\sigma_1}{F_1}\right)^2 - \left(\frac{1}{F_1^2} + \frac{1}{F_2^2}\right)\sigma_1\,\sigma_2 + \left(\frac{\sigma_2}{F_2}\right)^2 + \left(\frac{\sigma_6}{F_6}\right)^2 - 1$
2	Tsai-Hill yield criteria (Azzi & Tsai) [13]	$\left(\frac{\sigma_1}{F_1}\right)^2 - \left(\frac{\sigma_1\,\sigma_2}{F_1^2}\right) + \left(\frac{\sigma_2}{F_2}\right)^2 + \left(\frac{\sigma_6}{F_6}\right)^2 - 1$
3	(Norris&Mckinnon)[14]	$\left(\frac{\sigma_1}{F_1}\right)^2 + \left(\frac{\sigma_2}{F_2}\right)^2 + \left(\frac{\sigma_6}{F_6}\right)^2 - 1$
4	Norris distortional energy (Norris)[15]	$\left(\frac{\sigma_1}{F_1}\right)^2 - \left(\frac{\sigma_1\,\sigma_2}{F_1^2}\right) + \left(\frac{\sigma_2}{F_2}\right)^2 + \left(\frac{\sigma_6}{F_6}\right)^2 - 1$ $\left(\frac{\sigma_1}{F_1}\right)^2 - 1 \;;\; \left(\frac{\sigma_2}{F_2}\right)^2 - 1$
5	Hoffman Theory (Hoffman) [16]	$(\frac{\sigma_1^2}{F_{1t}F_{1c}}) + (\frac{\sigma_2^2}{F_{2t}F_{2c}}) - (\frac{\sigma_1\sigma_2}{F_{1t}F_{1c}}) + (\frac{F_{1c} - F_{1t}}{F_{1t}F_{1c}})\sigma_1 + (\frac{F_{2c} - F_{2t}}{F_{2t}F_{2c}})\sigma_2 + (\frac{\sigma_6}{F_6})^2 - 1$
6	(Tsai and Wu) [17]	$(\frac{1}{F_{1t}} - \frac{1}{F_{1c}})\sigma_1 + (\frac{1}{F_{2t}} - \frac{1}{F_{2c}})\sigma_2 + \frac{\sigma_1^2}{F_{1t}F_{1c}} + \frac{\sigma_2^2}{F_{2t}F_{2c}} + 2H_{12}\sigma_1\,\sigma_2 + (\frac{\sigma_6}{F_6})^2 - 1$ and $\frac{1}{F_{1t}F_{1c}} \cdot \frac{1}{F_{2t}F_{2c}} - H_{12}^2 \geq 0$ for stability
-	Tsai-Hahn[18]	The same criterion as tsai-Wu but the value of H_{12} is $H_{12} = -0.5\sqrt{\frac{1}{F_{1t}F_{1c}} \cdot \frac{1}{F_{2t}F_{2c}}}$
8	Cowin[19]	The same criterion as Tsai-Wu but the value of H_{12} is $H_{12} = \sqrt{\frac{1}{F_{1t}F_{1c}}} \cdot \sqrt{\frac{1}{F_{2t}F_{2c}}} - \frac{1}{2F_6^2}$

(a) If A/B < 2

The stress state is (tension-compression) i.e σ_1 and σ_2 have different signs and the experimental results show a close agreement with Tsai-Hahn criterion and the theories listed in Eq.2. This is not true in case of the other criteria.

(b) If A/B > 2

The stress state is (tension-tension) and (comp.-comp.) i.e. σ_1 and σ_2 have the same sign. The experimental results are not in agreement with any of the failure criteria. This was clear also in the results of M.J. Owen [5] in zero shear condition applied to several failure criteria as mentioned before. That is because the tensile stresses acting perpendicular and along the fibers in presence of the shear stress help the micro cracks to initiate and to propagate tangentially to the fibers. This is called the interfacial shear mode.

Although there is no analytical expression for the strength guarding against this kind of failure, it may be contributed to the analysis by using the Tsai-Wu theory in the form

$$(\frac{\sigma_1}{F_1})^2 + (\frac{\sigma_2}{F_2})^2 + (\frac{\sigma_6}{F_6})^2 + 2H_{12}\sigma_1\sigma_2 = 1 \quad (5)$$

Applying [45,-45] pure bending test will give the value of H_{12}

$$\text{then} \quad H_{12} = (\frac{2}{A^2} - \frac{1}{F_1^2} - \frac{1}{2F_6^2})$$

Where A is the amplitude of the global bending stress of [45,-45] pure bending test which is a function of N.

This value of stress interaction term which will be evaluated from experimental test combines the interfacial shear strength with the matrix shear strength and the fiber flexural strength.

Referring to Figures (9) to (14), the comparison between the S-N curves of in-phase and out-of-phase loading conditions was based on the same (A/B) ratio for the two curves. But, for out-of-phase loading the condition $\sigma_x = A$ and $\tau_{xy} = B$ will not exist in the same time. Thus, it was expected that out-of-phase loading will give longer life - for the same A and B- than the in-phase loading. But, this did not happen except when the stress level was low. And in contrast, at high stress levels for the same peaks of A and B the life under out-of-phase condition was shorter. This is because at high stress levels the stress is high enough to initiate cracks in the matrix and due to the out-of-phase condition, the plane of maximum stress is rotating through the cycle [20]. This rotation gives the chance to the crack to be subjected to the maximum stress at multi mode of loading. This leads to a higher speed of crack propagation and hence shorter lives were recorded. For low stress levels A and B were not acting in the same instant, so the local stresses in the matrix were not able to initiate cracks and then gave longer lives. These results are in agreement with F. Ellyin et al. [21]. They concluded that when the applied loads induce a plastic deformation (high strain), for the same strain amplitude, the fatigue life decreases with increase of the phase angle . However, for strain amplitudes less than certain level the fatigue life of out-of-phase tests (Z = 60 deg., 90 deg.) is much longer than that of in-phase test. Figures (17) and (18) represent constant life diagrams for [0,90] and [45,-45] tubes respectively to compare between in-phase and out-of-phase loading conditions.

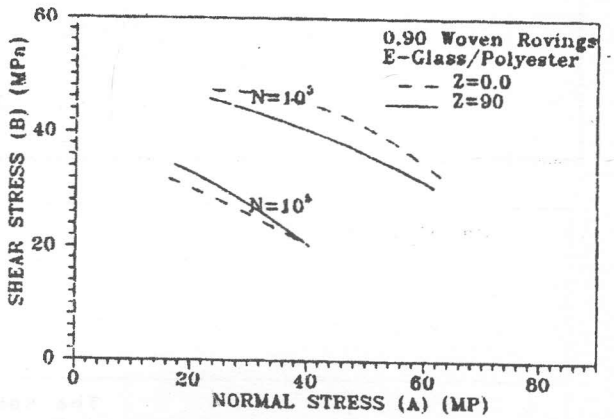

Figure 17. Comparison between failure contours of 0,90 GRP in-phase and out-of-phase.

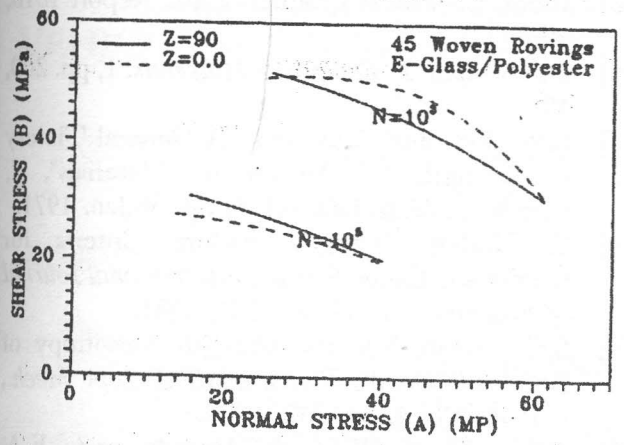

Figure 18. Comparison between in-phase and out-of-phase failure contours of 45,-45 woven roving GRP.

CONCLUSION

The failure criteria applied to woven roving GRP tubes under combined bending and torsional moments may be used safely with [0,90] configuration. In this case only two fatigue tests are required, pure bending of [0,90] to get F_1, and pure torsion of [0,90] to get F_6.

For [45,-45] tubes, if A/B $\leq$ 2 the Tsai-Hahn criterion is relatively closer and may be applied in the form

$$(\frac{\sigma_1}{F_1})^2 + (\frac{\sigma_2}{F_2})^2 + (\frac{\sigma_6}{F_6})^2 + 2H_{12}\sigma_1\sigma_2 = 1$$

where

$$H_{12} = \frac{-0.5}{F_1^2}$$

But, if A/B > 2 the interaction term has to be changed. Its new expression and value needs another test. This test is pure bending of [45,-45] composites.

This gives

$$H_{12} = (\frac{2}{A^2} - \frac{1}{F_1^2} - \frac{1}{2F_6^2})$$

where A is the amplitude of the global bending strength of the [45,-45] pure bending test.

For out-of-phase loading conditions, as the stress level increases the decrease in fatigue life is much higher than that for in-phase loading condition. Yet, no formula has been found and it needs more experiments with several phase angles. But for lives more than 20000 cycles, the out-of-phase conditions give longer lives compared with that recorded for in-phase conditions. Hence, ignoring its presence will not be dangerous.

6. REFERENCES

[1] R.M. Jones, *Mechanics of Composite Materials*, McGraw-Hill, Kogakusha, Ltd. 1975.

[2] P.H. Francis, D.E. Walrath, D.S. Sims, and D.N. Weed, "Biaxial Fatigue Loading of Notched Composites", *J. Composite Materials*, vol. 11, pp. 488, Oct. 1977.

[3] R.L. Daugherty, "Composite Leaf Spring in Heavy Truck Applications", Composite Materials, K. Kawata and T. Akasaka, E.D., *Proc. Japan-U.S. Conference*, Tokyo, 1981.

[4] P.C. Chow, "A cumulative Damage Rule for Fatigue of Composite Materials", AFML-TR, Wright-Patterns on Air Force Base, Ohio54533.

[5] M.J. Owen, J.R. Griffiths, "Evaluation of Biaxial Stress Failure Surfaces for a Glass Fabric Reinforced Polyester Resin Under Static and Fatigue -Loading", *J. of Mat. Sci.* vol. 13, n.7, p 1521, Jul. 1978.

[6] M.J. Owen and D.J. Rice, "Biaxial Strength Behaviour of Glass Fabric - Reinforced Polyester Resins", Composites, pp. 13-25, Jan. 1981.

[7] R.R. Rizzo And A.A. Vicario, "A Finite Element Analysis of Laminated Anisotropic Tubes", *J. Composite Materials*, vol. 4, July 1970.

[8] A.A. Vicario And R.R. Rizzo, "Effect of Length on Laminated Thin Tubes Under Combined Loading", *J. Composite Materials.* vol. 4, pp. 274, April 1970.

[9] S.S. Wang, E.S. - Chim, D.F. Socie, J.V. Gauchel and, J.L. Olinger, "Tensile and Torsional Fatigue of Fiber-Reinforced Composites at Gryogenic Temperatures", *J. of*

Eng. Mat. and Tech., vol. 104, Ppp. 121, April 1982.

[10] M.N. Aboul Wafa, A. Hamdy and, E.A. Showaib, "A New Testing Machine for Fatigue Under Combined Bending and Torsion Acting out of Phase", Alex. Eng. *J., Alex. Univ.*, vol. 28, No.4, pp. 113, 1989.

[11] P.D. Herrington, A.B. Doucet, J.E. Beard, and M. Sabbaghian, "Study of Delamination Damage around a Discontinuity in Composite Bending Fatigue Specimens", Advanced Materials: Looking Ahead to the 21st Century *National SAMPE Technical Conference*, V22, Pub. by SAMPE, Covina, CA, USA, pp. 834, 1990.

[12] R. Hill, *Proc. Roy. Soc.* A 193, pp. 281, A 193 1948.

[13] V.D. Azzi and S.W. Tsai, EXP. Mech. 5, pp. 283, 1965.

[14] C.B. Norris and P.F. McKinnon, US Forest Products Lab., Report 1328, 1956.

[15] Idem, US Forest Products Lab., Report 181(1962.

[16] O.Hoffman, *J. Composite Materials*, 1, pp. 20(1967.

[17] S.W. Tsai and E.M. Wu, "A General Theor of Strength for Anisotropic Materials", J *Composite Materials*, vol. 5, pp. 58,Jan. 1971.

[18] Z. Hashin, "Fatigue Failure Criteria fc Combined Cyclic Stress", *International Journa of Fracture,* vol. 17, pp. 101, 1981.

[19] S.C. Cowin, "On the strength Anisotropy c Bone and Wood", Trans. *ASME J. Appl. Mech* vol. 46, No. 4, pp. 832, 1979.

[20] M.N. Aboul Wafa, A. Hamdy and, E.A Showaib, "Analytical Study to the out of phas(combined Bending and Torsional Stresses" Alex. Eng. *J., Alex. Univ.*, vol. 28, No, pp 131, Oct. 1989.

[21] F. Ellyin and Z. Xia, "A General Fatigu(Theory and its Application to Out-of-Phase Cyclic Loading", *J. of Eng. Mat. and Tech.* vol. 115, pp. 411, Oct. 1993.